

Electrochemical Determination of Acetylsalicylic acid in Human Urine Samples Based on Poly (diallyldimethylammonium chloride) Functionalized Reduced Graphene Oxide Sheets

Hang Zhu

Putian Univeristy, Dong Zhen West Road No. 450, Putian City, Fujian Province, 351100, P.R.China;
E-mail: hangzhupt@gmail.com

Received: 21 January 2016 / Accepted: 23 February 2016 / Published: 1 April 2016

In this contribution, a poly (diallyldimethylammonium chloride) functionalized reduced graphene oxide (PDDA-RGO) was synthesized via a simple one-pot hydrothermal approach using urea as reducing agent. The synthesized PDDA-RGO was carefully characterized via various techniques including scanning electron microscopy, transmission electron microscopy, X-ray powder diffraction, Raman spectroscopy and Fourier transform infrared spectroscopy. The synthesized PDDA-RGO was then used as an electrode surface modifier for electrochemically determination of acetylsalicylic acid. Cyclic voltammetry and differential pulse voltammetry were used as determination techniques. Various determination parameters were optimized as well. Moreover, the application of the proposed sensor was successfully applied for acetylsalicylic acid determination in human urine samples.

Keywords: Graphene; PDDA; Electrochemical; Acetylsalicylic acid; Sensor

1. INTRODUCTION

Acetylsalicylic acid, acetylsalicylic acid, is the prototype of the salicylates, which is widely used as an antiseptic agent, antiinflammatory agent, germicide and antipyretic in clinical and pharmaceutical industry. It showed very promise curative effect in many kinds of degenerative diseases including certain types of cancer, senile cataracts and cardiovascular and cerebrovascular diseases. It can be also used as a pain killer and fever reliever. Due to the widespread use of this drug, overdose become a serious problem. Therefore, development of a reliable method for acetylsalicylic acid detection is essential. To date, different approaches have been successfully proposed for detecting acetylsalicylic acid and its related metabolites. These methods including high-performance liquid

chromatography (HPLC) [1], UV-Vis spectrometry [2], spectrofluorimetry [3], flow injection analysis [4] and fluorescence detection [5]. Each of these methods has its own advantages as well as its limitations. For example, HPLC operation requires highly trained technical staff. The instrument of the flow injection analysis is expensive. In contrast, electrochemical approach is an alternative way for acetylsalicylic acid detection due to its simplicity, low-cost, high accuracy and low detection limit. However, acetylsalicylic acid is weak electrochemical active material, common electrode cannot be used for effectively detection. Accordingly, this area remains a large challenge to construct a simple, low-cost, high sensitivity electrochemical sensor for acetylsalicylic acid determination in biological fluids.

Graphene is a 2-dimensional single carbon atoms network, which got lots of attentions after it has been isolated from graphite in 2004 [6]. Graphene has been found many distinct properties such as outstanding electronic conductivity, extreme large surface area and superior electrocatalytic performance. Many studies already showed the graphene could serve as an excellent electrode surface modifier for constructing electrochemical sensors [7-13]. However, graphene has poor dispersibility in many kinds of solvents, which make it harder to interact with other substances. In order overcome this problem, poly (diallyldimethylammonium chloride) (PDDA) has been used for functionalizing graphene. Recent study showed the PDDA is capable for reducing graphene oxide (GO), an oxide form of graphene, under hydrothermal condition. Based on the excellent solubility of the GO, we expect the PDDA functionalized reduced GO (RGO) could serve as a promise electrode surface modifier for acetylsalicylic acid detection.

In this work, we prepared a PDDA functionalized RGO (PDDA-RGO) using a simple and facial one-pot hydrothermal method using urea as reducing agent. As-synthesized PDDA-RGO was characterized using different techniques to confirm the formation and analysis of its properties. Subsequently, a sensitive electrochemical sensor for acetylsalicylic acid detection was fabricated by PDDA-RGO modified glassy carbon electrode (GCE).

2. EXPERIMENTS

2.1 Chemicals and materials

Acetylsalicylic acid, synthetic graphite (average diameter $<30\ \mu\text{m}$), poly (diallyldimethylammonium chloride) (20 wt. % in H_2O), glucose, urea, ascorbic acid were purchased from Sigma-Aldrich and used without further purification. KH_2PO_4 and K_2HPO_4 were used for making phosphate buffer solution (PBS).

2.2 GO synthesis

Graphene oxide (GO) was prepared with the modified Hummers method with little modification [14, 15]. Briefly, graphite (4 g) was added into 100 mL of concentrated H_2SO_4 and followed adding 2.5 g NaNO_3 . Then, KMnO_4 (15 g) was added into the above solution under stirring.

The reaction was maintained below 20 °C. 200 mL water was then slowly added into above solution until boiling and maintained at this state for half hour and then stopped by adding excess water and H₂O₂ solution. Low concentration of HCl was used for washing sample. BaCl₂ was used as indicator for determining the sample was neutralized. Then, the solid sample was centrifuged and dried in an oven. The surface negatively charged oxygen containing groups on GO make it could simply disperse into water.

2.3 PDDA-RGO synthesis

PDDA-RGO was synthesized using a one-pot hydrothermal approach. Briefly, 2 mL PDDA was added into 10 mL GO (1 mg/mL) and went 2 h bath sonication. 20 mg urea was then added into the mixture and further sonicate for 1 h. The whole mixture was then transferred into a 50 mL Teflon-lined stainless steel autoclave. The autoclave was then heated at 120 °C for 10 h. After naturally cool down, the result dispersion was centrifuged at washed by water and ethanol twice. RGO without PDDA functionalization was also prepared using a similar approach except adding PDDA.

2.4 Characterization

The structure and morphology of the sample was studied by a scanning electron microscopy (SEM, ZEISS, SUPRA 55) and a transmission electron microscopy (TEM, JEOL JEM-2100). The crystal phase information of the sample was studied by a X-ray powder diffraction (XRD, Bruker, D8-Advanced) in the 2 θ of 5° to 60° using Cu K α ($\lambda = 0.1546$ nm) radiation. A Raman spectroscopy with 514 nm laser light (Renishaw, RM1000) was also used for analyzing carbon crystal state of the samples. UV-vis spectroscopy was used for analysis of optical property of samples. Fourier transform infrared spectroscopy (FTIR, Thermo Scientific, Nicolet iS5) was used for analyzing surface functional groups of the samples. Thermogravimetric analysis (TGA, Netzsch TG 209) of samples was tested in N₂ condition from 30 to 700 °C with a heating rate of 10 °C/min.

2.5 Electrochemical measurement of acetylsalicylic acid

For electrochemical measurement, a glassy carbon electrode (GCE) was polished by different size of alumina powder dispersion. The GCE surface modification was according to following procedures: 5 μ L modifier dispersion (1 mg/mL) was dropped on the GCE surface and the solvent was evaporated in a fume hood. The electrochemical determination experiments were carried out at an electrochemical workstation (CHI 660a) using three electrodes system, which a GCE as working electrode, a platinum electrode as the auxiliary electrode and an Ag/AgCl (3M KCl) as the reference electrode. Bare GCE (without any modification) was used as the control group. RGO dispersion and PDDA-RGO dispersion were used for modifying the GCE surface and denoted as RGO/GCE and PDDA-RGO/GCE, respectively. The CV measurements were carried out at scan range between 0.4-1.1 V with scan rate of 50 mV/s. The EIS measurements were carried out in 0.1 M PBS (pH = 8.0)

containing 5 mM $\text{Fe}(\text{CN})_6^{3-/4-}$ (1:1) with 0.1 M KCl. The DPV measurements were carried out at scan range between 0.5-1.0 V. The modulation time was set as 0.05s with a time interval of 0.2s and a step potential of 0.2mV/s. The accumulation potential measurements were carried out at the 0.1 M PBS with 1 mM acetylsalicylic acid using different constant potentials. For interference study, different interference species including glucose, 4-nitrophenol, paracetamol, uric acid ascorbic acid and H_2O_2 were added into the PBS containing 1 mM acetylsalicylic acid. DPV method was then conducted for current response measurement.

3. RESULTS AND DISCUSSION

3.1 Characterization of PDDA-RGO

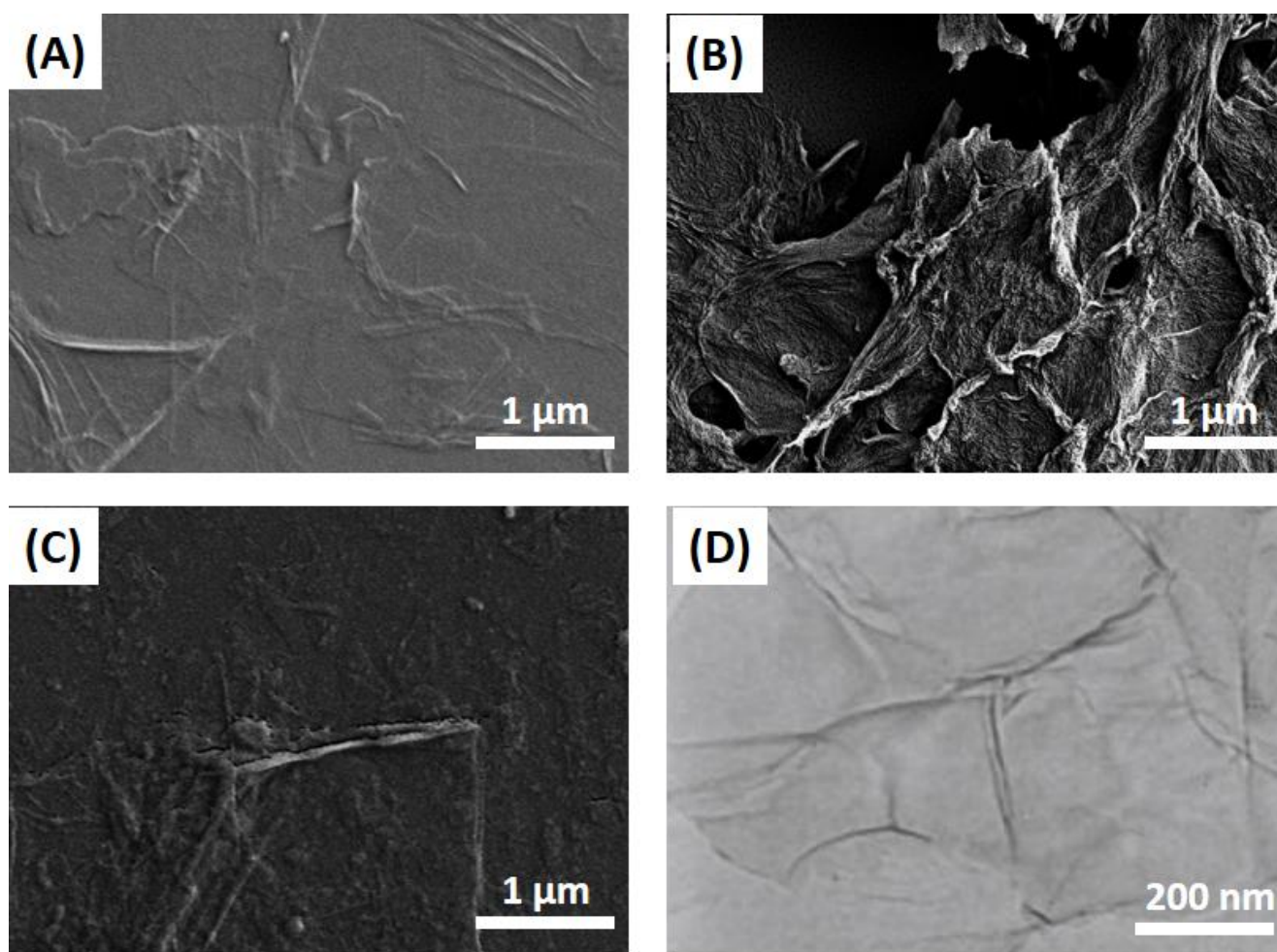


Figure 1. SEM images of (A) GO, (B) RGO and (C) PDDA-RGO. TEM image of (D) PDDA-RGO.

The structure and morphology of GO, RGO and PDDA-RGO was analysed using SEM. Figure 1a-c shows the SEM observations of GO, RGO and PDDA-RGO samples. It can be seen that the GO (Figure 1A) shows sheet like winkle structure and well dispersibility on the substrate without any aggregation. After chemical reduction process, RGO (Figure 1B) exhibits obvious re-stacking effect due to the loss of surface negatively charges. The re-stacking effect could highly reduce the specific

surface area of the material, which provides less chance for interacting with other substances. In contrast, PDDA-RGO (Figure 1C) remains a well dispersibility without clear re-stacking effect due to the surface protection of PDDA. The presence of PDDA not only could prevent the natural force of graphene layers stacking together, its surface positive charges also provide repulsion between the sheets, which is favourable for forming a stable suspension. The fine morphology of the PDDA-RGO was also observed using TEM and presents in Figure 1D. The observation of PDDA-RGO showed a general flake-like structure of graphene, indicating the surface functionalization did not change the morphology of the graphene.

The reduction of GO was firstly confirmed using UV-vis spectroscopy. As shown in Figure 2A, the UV-vis spectrum of GO shows a characteristic absorbance peak located at 230 nm, which ascribed to π - π^* transitions of aromatic C—C bonds [16].

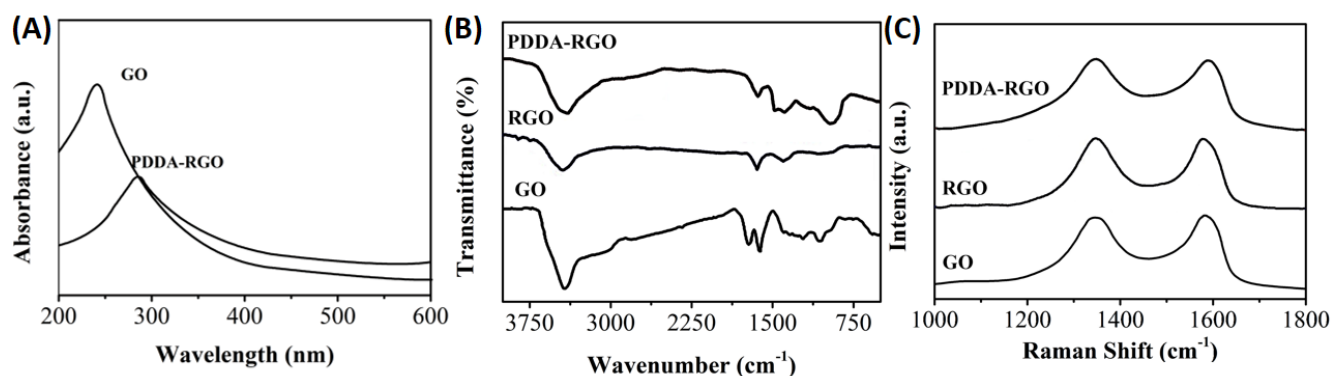


Figure 2. (A) UV-vis spectra of GO and PDDA-RGO. (B) FTIR spectra and (C) Raman spectra of GO, RGO and PDDA-RGO.

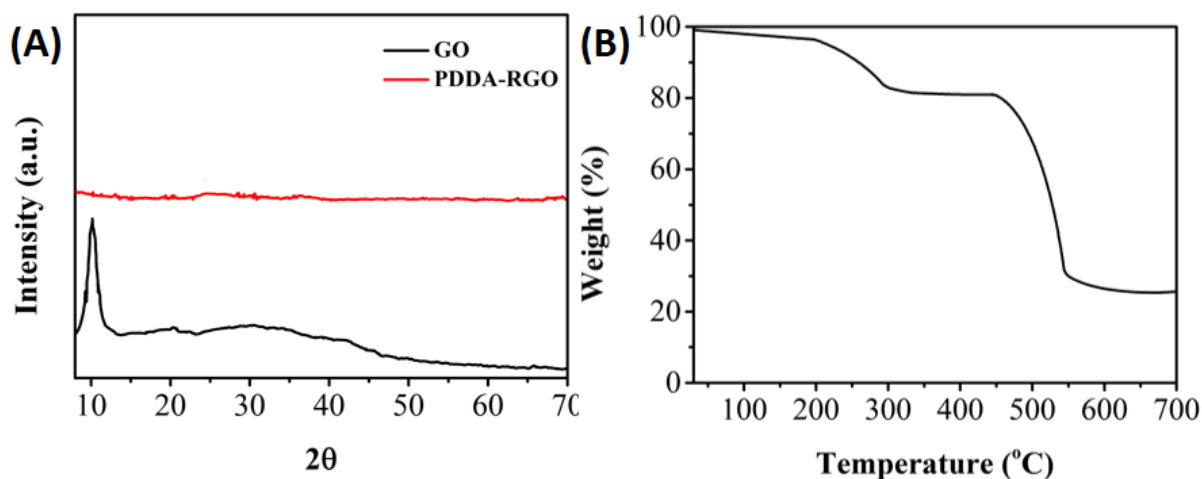


Figure 3. (A) XRD pattern of GO and PDDA-RGO. (B) TGA curve of PDDA-RGO.

After reduced by urea under hydrothermal condition, this peak shifted to 271 nm, indicating the surface oxygen containing group removal. The reduction of GO was also confirmed by FTIR study. Figure 2B shows the FTIR spectra of GO, RGO and PDDA-RGO. A series of characteristic peaks were observed on the GO. The peaks at 1718, 1589, 1420 and 1030 cm⁻¹ can be assigned to the COOH

groups of C=O vibration, C=C stretching, C—OH mode vibration and C—O stretching, respectively [17-19]. After urea reduction under hydrothermal condition, the spectrum of RGO showed much weaker intensity of these characteristic peaks, some of these peaks even vanished, suggesting the GO indeed reduced. On the other hand, two new peaks located at 833 and 1510 cm^{-1} can be observed at the FTIR spectrum of PDDA-RGO sample, corresponding to the N—C bond present in PDDA molecules, suggesting the successful surface functionalization process [20, 21].

Because Raman spectroscopy is highly sensitive to the carbon state, thus provide a clear characterization for analysis the change of the GO. Figure 2C shows the Raman spectra of GO, RGO and PDDA-RGO. Two characterization peaks located around 1568 and 1337 cm^{-1} were clearly observed in the three spectra. The first peak (G band) can be ascribed to the graphite band, which due to the first-order scattering of E_{2g} phonons by sp^2 carbon atoms. The second peak (D band) can be ascribe to the diamondoid band, which due to the breathing mode of κ -point photons of A_{1g} symmetry [22-25]. The intensity ratio of two band can be used for analyzing the carbon state of graphene. As shown in the figure, the intensity ratio between D band and G band increases after urea reduction process, further suggesting the GO has been reduced under hydrothermal condition using urea as reducing agent [26]. Moreover, the G band of PDDA-RGO exhibits a small blue-shift, indicating the electron transfer from RGO to the adsorbed PDDA [20, 27-29].

Figure 3 A displays the XRD pattern of GO and PDDA-RGO. As observed in the figure, the GO displays a characteristic peak located at 11.2° with an interlayer spacing of 0.77 nm [30]. After reduction by urea under hydrothermal condition, this peak shifted to 22.9° , further confirming the successful removal of surface oxygen containing groups [31]. Figure 3B shows thermogravimetric curve of PDDA-RGO. A small weight loss was observed below 100°C due to the water evaporation. Weight loss between 200 to 300°C can be ascribed to the decomposition of PDDA. The major weight loss was observed at the temperature range between 450 to 550°C , corresponding to the decomposition of RGO to amorphous carbon.

3.2 Electrochemical determination of acetylsalicylic acid using PDDA-RGO modified GCE

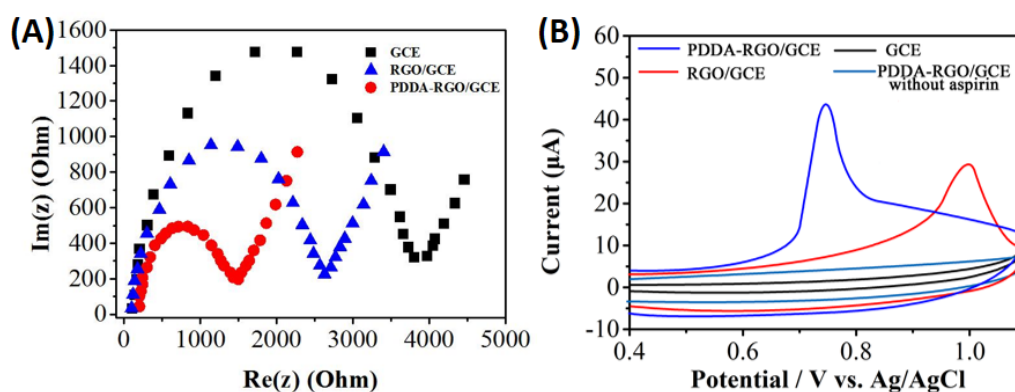


Figure 4. (A) Electrochemical impedance spectra of bare GCE, RGO/GCE and PDDA-RGO/GCE in 5 mM $\text{K}_3\text{Fe}(\text{CN})_6 + 0.1$ M KCl solution. (B) CVs recorded at a bare GCE, RGO/GCE and PDDA-RGO/GCE with 1 mM acetylsalicylic acid and without acetylsalicylic acid in the 0.1 M PBS (pH 7.0). Scan rate: 50 mV/s

The electron transfer ability of bare GCE, RGO and PDDA-RGO modified GCE was investigated by and electrochemical impedance spectroscopy (EIS). Figure 4A shows the Nyquist plots of bare GCE, RGO and PDDA-RGO. It can be seen that the bare GCE shows the largest semicircle, indicating the bare GCE owing the highest electron transfer resistance. After modification with RGO, the RGO/GCE shows a smaller semicircle than that of bare GCE, indicating the increased electron transfer performance due to the excellent electro-conductivity. In contrast, the PDDA-RGO/GCE shows a further decreasing of semicircle diameter, indicating the PDDA surface functionalization prevented the re-stacking effect of the graphene, which could further lower the electron transfer resistance of the electrode. The differences of the EIS performance in three electrodes indicate the PDDA-RGO may have the higher electro-conductivity due to the fast electron transfer rate.

Figure 4B displays the CV profiles of bare GCE, RGO and PDDA-RGO modified GCE toward detection of 1 mM acetylsalicylic acid at scan rate of 50 mV/s. It can be seen that the GCE shows on clear oxidation peak in the scan range, indicating the acetylsalicylic acid cannot oxidase in this potential range using commercial GCE. While at RGO/GCE, a clear oxidation peak can be observed in the potential of 0.98 V with 32 μA . This current response can be ascribed to the excellent conductivity and electrocatalytic activity of RGO. In contrast, the PDDA-RGO/GCE shows a further decreasing of over potential with higher current response, suggesting the PDDA surface functionalization not only further lower the electron transfer resistance of the electrode but also enhance the electrocatalytic property of the modifier. Based on the EIS and CV characterizations, the enhancement of the electrochemical activity of PDDA-RGO modified GCE was confirmed.

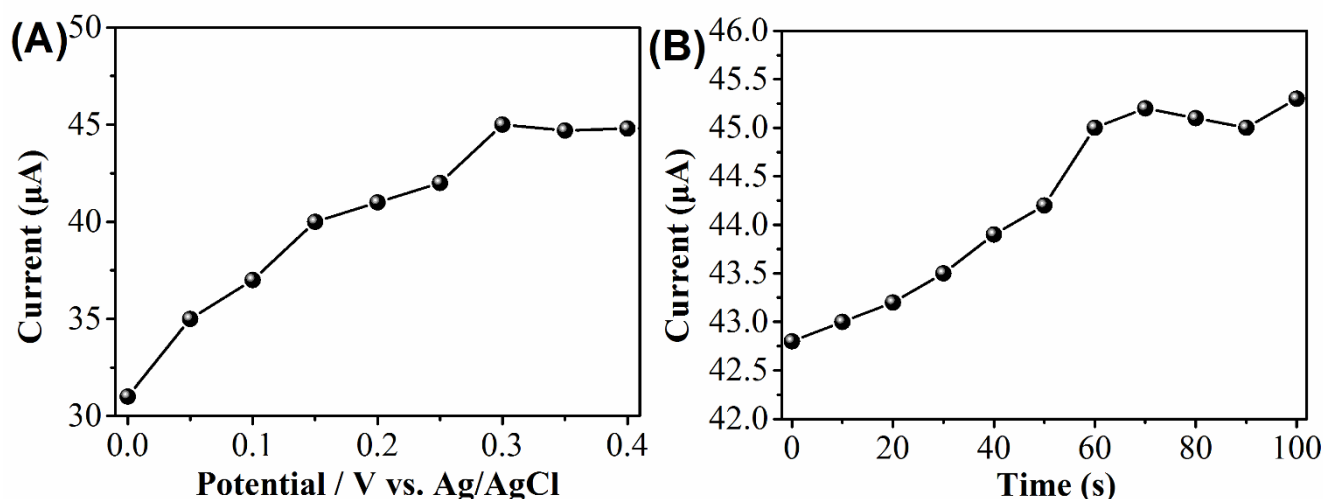


Figure 5. Effects of (A) accumulation potential and (B) time on PDDA-RGO/GCE in 1 mM acetylsalicylic acid in the 0.1 M PBS (pH 7.0).

In order to optimize the detection parameters, we investigated the effect of accumulation potential and period. As shown in Figure 5A, the accumulation potential could greatly affect the final current response. As can be seen that the current response gradually increases from 0 to 0.3 V and then reaches to the maximum. Therefore, 0.3 V was chosen as optimized accumulation potential. On the other hand, accumulation time also could clearly affect the current responses. As shown in Figure 5B,

the current response increased from 0 to 60 s and then remained in a same level. Therefore, we chose 60 s as accumulation time in this study.

Differential pulse voltammetry (DPV) was employed for determining acetylsalicylic acid under the optimum experimental conditions due to its high sensitivity and selectivity compared with CC. As shown in the Figure 6, the oxidation current response of the PDDA-RGO/GCE gradually increases along with the acetylsalicylic acid concentration increasing from 5 μM to 2 mM. The obtained linear equation can be expressed as $I (\mu\text{A}) = 0.2487C (\mu\text{M}) + 6.4175$ ($R^2 = 0.9984$). Based on the signal to noise of 3, the detection limit of the PDDA-RGO/GCE towards acetylsalicylic acid can be estimated as 1.17 μM . Table 1 shows the comparison of our proposed acetylsalicylic acid sensor with several reported electrochemical sensors. Results showed that theour proposed PDDA-RGO/GCE had a superior performance towards acetylsalicylic acid detection, especially had a wide detection range. Therefore, our proposed acetylsalicylic acid electrochemical sensor can be potentially used for practical application.

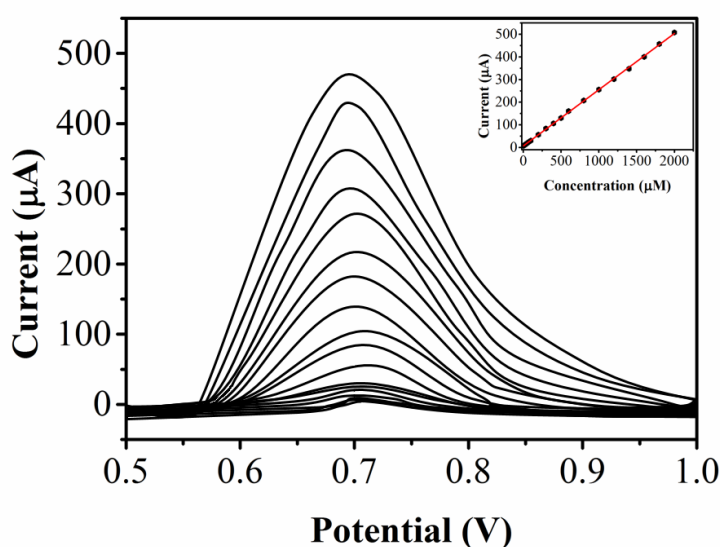


Figure 6. DPV curves of the PDDA-RGO towards addition of acetylsalicylic acid (5-2000 μM) in the 0.1 M PBS (pH 7.0). Inset: calibration curve of concentrations of acetylsalicylic acid and current responses. Modulation time: 0.05s; time interval: 0.2s; step potential: 0.2mV/s.

Table 1. Comparison of our proposed acetylsalicylic acid electrochemical sensor with other reports.

Electrode	Linear range (μM)	Limit of detection (μM)	Reference
Triton X 100-carbon nanotube	2.61-627	0.258	[32]
Pyrolytic graphite electrode	0.02-100	0.016	[33]
PATP-AuNPs	0.001-0.1	0.0003	[34]
Cobalt hydroxide	100-700	62.8	[35]
PDDA-RGO/GCE	5-2000	1.17	This work

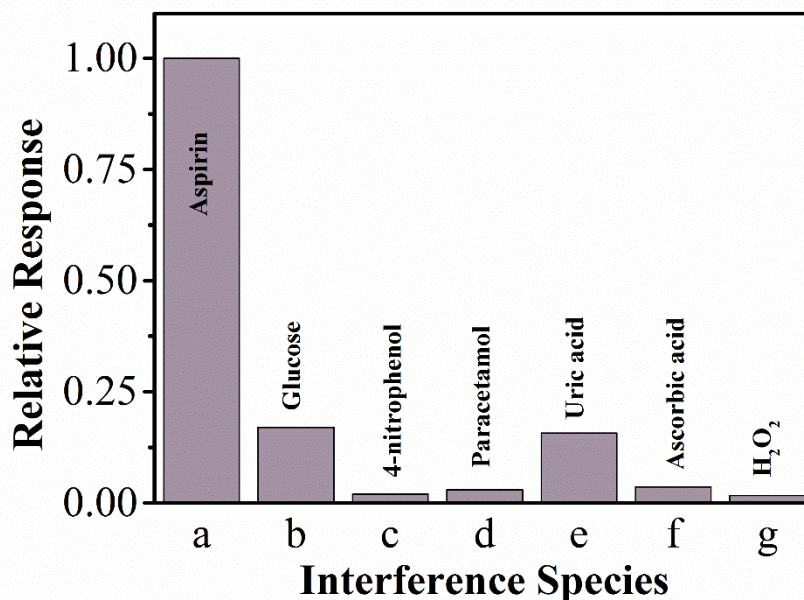


Figure 7. Anti-interference test using PDDA-RGO/GCE in 0.1 M PBS (pH 7.0).

Table 2. Determination of acetylsalicylic acid in tablets and urine samples using PDDA-RGO/GCE.

Sample	Spiked (μM)	Found (μM)	Recovery (%)	RSD (%)
Tablet 1	50	50.7	101.4	0.71
Tablet 2	100	99.4	99.4	0.44
Tablet 3	200	202.6	101.3	0.39
Tablet 4	500	497.3	99.5	0.25
Urine 1	50	50.9	101.8	0.33
Urine 2	100	98.5	98.5	0.27
Urine 3	200	203.4	101.7	0.88
Urine 4	500	504.5	100.9	0.91

The anti-interference property of the proposed acetylsalicylic acid electrochemical sensor was then studied. As shown in Figure 7, 10-fold concentrations of glucose, 4-nitrophenol, paracetamol, uric acid, ascorbic acid, H_2O_2 have no influence on the detection performance of the sensor towards acetylsalicylic acid (deviation below 10%). Therefore, our proposed PDDA-RGO/GCE can be selectively used for the determination of acetylsalicylic acid.

The stability test of our proposed acetylsalicylic acid electrochemical sensor was performed by 10 successive determinations of 1 mM acetylsalicylic acid in PBS. Results showed that the detection current decreased by about 7.2%, indicating that the sensor has acceptable stability.

In order to evaluate the practical performance of the proposed sensor, the fabricated PDDA-RGO/GCE was used to determine acetylsalicylic acid in human urine samples and tablets. For the urine sample test, the recoveries were investigated by spiking drug-free urine with known amounts of acetylsalicylic acid. The results are summarized in Table 2. The recovery obtained was in the range

from 97.6% to 104.1 %, indicating the proposed sensor could be successfully used for practical applications.

4. CONCLUSIONS

In summary, PDDA functionalized RGO was achieved under hydrothermal condition using urea as reducing agent. This method is simple and could be scaled up. The surface functionalization and reduction of GO were confirmed using a series techniques including UV-vis spectroscopy, Raman spectroscopy and FTIR. The prepared PDDA-RGO was then used as an electrode surface modifier for GCE modification. The fabricated PDDA-RGO/GCE was successfully used for electrochemically acetylsalicylic acid detection. Except the excellent detection performance, the proposed sensor also successfully applied for tablets and urine tests.

References

1. P. Virani, R. Sojitra, H. Raj and V. Jain, *Asian Journal of Pharmaceutical Analysis*, 5 (2015) 151
2. G. Bahrami, B. Mohammadi, S. Mirzaeei and A. Kiani, *Journal of Chromatography B*, 826 (2005) 41
3. H. M Maher, M. AA Ragab and E. I El-Kimary, *Combinatorial chemistry & high throughput screening*, 18 (2015) 723
4. J.S. Stefano, R.H. Montes, E.M. Richter and R.A. Muñoz, *Journal of the Brazilian Chemical Society*, 25 (2014) 484
5. M.A. Husain, S.U. Rehman, H.M. Ishqi, T. Sarwar and M. Tabish, *RSC Advances*, 5 (2015) 64335
6. K.S. Novoselov, A.K. Geim, S.V. Morozov, D. Jiang, Y. Zhang, S.V. Dubonos, I.V. Grigorieva and A.A. Firsov, *Science*, 306 (2004) 666
7. L. Fu, Y. Zheng and A. Wang, *Int. J. Electrochem. Sci*, 10 (2015) 3518
8. Y. Zheng, L. Fu, A. Wang and W. Cai, *Int. J. Electrochem. Sci*, 10 (2015) 3530
9. F. Han, H. Li, J. Yang, X. Cai and L. Fu, *Physica. E*, 77 (2016) 122
10. L. Fu, G. Lai and A. Yu, *RSC Advances*, 5 (2015) 76973
11. L. Fu, S. Yu, L. Thompson and A. Yu, *RSC Advances*, 5 (2015) 40111
12. Y. Zheng, A. Wang, H. Lin, L. Fu and W. Cai, *RSC Advances*, 5 (2015) 15425
13. L. Fu, Y. Zheng, A. Wang, W. Cai, Z. Fu and F. Peng, *Sensor Letters*, 13 (2015) 81
14. W.S. Hummers and R.E. Offeman, *Journal of the American Chemical Society*, 80 (1958) 1339
15. T. Gan and S. Hu, *Microchim. Acta.*, 175 (2011) 1
16. J.I. Paredes, S. Villar-Rodil, A. Martínez-Alonso and J.M.D. Tascón, *Langmuir*, 24 (2008) 10560
17. J. Zhang, H. Yang, G. Shen, P. Cheng, J. Zhang and S. Guo, *Chemical Communications*, 46 (2010) 1112
18. M. Ahmad, E. Ahmed, Z.L. Hong, J.F. Xu, N.R. Khalid, A. Elhissi and W. Ahmed, *Appl. Surf. Sci.*, 274 (2013) 273
19. X. Li, Q. Wang, Y. Zhao, W. Wu, J. Chen and H. Meng, *Journal of colloid and interface science*, 411 (2013) 69
20. S. Wang, D. Yu, L. Dai, D.W. Chang and J.-B. Baek, *ACS Nano*, 5 (2011) 6202
21. L. Fu, Y. Zheng, Q. Ren, A. Wang and B. Deng, *Journal of Ovonic Research*, 11 (2015) 21
22. Z.-J. Fan, W. Kai, J. Yan, T. Wei, L.-J. Zhi, J. Feng, Y.-m. Ren, L.-P. Song and F. Wei, *ACS Nano*,

- 5 (2010) 191
23. L. Fu and Z. Fu, *Ceram Int*, 41 (2015) 2492
24. L. Fu, W. Cai, A. Wang and Y. Zheng, *Materials Letters*, 142 (2015) 201
25. L. Fu, A. Wang, Y. Zheng, W. Cai and Z. Fu, *Materials Letters*, 142 (2015) 119
26. L.L. Zhang, R. Zhou and X.S. Zhao, *Journal of Materials Chemistry*, 20 (2010) 5983
27. A.M. Rao, P.C. Eklund, S. Bandow, A. Thess and R.E. Smalley, *Nature*, 388 (1997) 257
28. X. Qi, K.-Y. Pu, X. Zhou, H. Li, B. Liu, F. Boey, W. Huang and H. Zhang, *Small*, 6 (2010) 663
29. M.-C. Hsiao, S.-H. Liao, M.-Y. Yen, P.-I. Liu, N.-W. Pu, C.-A. Wang and C.-C.M. Ma, *ACS applied materials & interfaces*, 2 (2010) 3092
30. T. Nakajima, A. Mabuchi and R. Hagiwara, *Carbon*, 26 (1988) 357
31. D. Miao, J. Li, R. Yang, J. Qu, L. Qu and P.d.B. Harrington, *Journal of Electroanalytical Chemistry*, 732 (2014) 17
32. P. Phukon, K. Radhapyari, B.K. Konwar and R. Khan, *Materials Science and Engineering: C*, 37 (2014) 314
33. R.N. Goyal, S. Bishnoi and B. Agrawal, *Journal of Electroanalytical Chemistry*, 655 (2011) 97
34. Z. Wang, H. Li, J. Chen, Z. Xue, B. Wu and X. Lu, *Talanta*, 85 (2011) 1672
35. M. Houshmand, A. Jabbari, H. Heli, M. Hajjizadeh and A. Moosavi-Movahedi, *Journal of Solid State Electrochemistry*, 12 (2008) 1117

© 2016 The Authors. Published by ESG (www.electrochemsci.org). This article is an open access article distributed under the terms and conditions of the Creative Commons Attribution license (<http://creativecommons.org/licenses/by/4.0/>).